Neoplasia • Vol. 1, No. 4, October 1999, pp. 303–310 303

Available On-line at http://www.neoplasia.org

Noninvasive Assessment of Tumor Cell Proliferation in Animal Models

Matthias Edinger, Thomas J. Sweeney*, Amanda A. Tucker*, Adesuwa B. Olomu†, Robert S. Negrin* and Christopher H. Contag†*

*Department of Medicine, Stanford University School of Medicine, Stanford, CA 94305-5623; †Department of Pediatrics, Stanford University School of Medicine, Stanford, CA 94305-5208

Abstract

Revealing the mechanisms of neoplastic disease and enhancing our ability to intervene in these processes requires an increased understanding of cellular and molecular changes as they occur in intact living animal models. We have begun to address these needs by developing a method of labeling tumor cells through constitutive expression of an optical reporter gene, and noninvasively monitoring cellular proliferation *in vivo* using a sensitive photon detection system. A stable line of HeLa cells that expressed a modified firefly luciferase gene was generated, and proliferation of these cells in irradiated severe combined immunodeficiency (SCID) mice was monitored. Tumor cells were introduced into animals via subcutaneous, intraperitoneal and intravenous inoculation and whole body images, that revealed tumor location and growth kinetics, were obtained. The number of photons that were emitted from the labeled tumor cells and transmitted through murine tissues was sufficient to detect 1×10^3 cells in the peritoneal cavity, 1×10^4 cells at subcutaneous sites and 1×10^6 circulating cells immediately following injection. The kinetics of cell proliferation, as measured by photon emission, was exponential in the peritoneal cavity and at subcutaneous sites. Intravenous inoculation resulted in detectable colonies of tumor cells in animals receiving more than 1×10^6 cells. Our demonstrated ability to detect small numbers of tumor cells in living animals noninvasively suggests that therapies designed to treat minimal disease states, as occur early in the disease course and after elimination of the tumor mass, may be monitored using this approach. Moreover, it may be possible to monitor micrometastases and evaluate the molecular steps in the metastatic process. Spatiotemporal analyses of neoplasia will improve the predictability of animal models of human disease as study groups can be followed over time, and this method will accelerate development of novel therapeutic strategies.

Keywords: luciferase, noninvasive monitoring, cancer, tumor progression, imaging, *in vivo*, therapy.

Introduction

Development of neoplastic disease is a complex process involving the loss of genetic and immune regulation, as well as interactions between the transformed cells and surrounding tissues. Therefore, it is essential to evaluate the processes of cell transformation and tumor growth in the context of the intact organ systems of living animals. New tools that can noninvasively assess the molecular and cellular events leading to the generation and proliferation of transformed cells are necessary. Several advanced imaging strategies that utilize fluorescence imaging, magnetic resonance imaging (MRI) and positron emission tomography (PET), have been described for the study of neoplastic disease [1–11]. However, a versatile, rapid and sensitive assay that is inexpensive and that reveals cellular and molecular changes as they occur in intact animal models of human neoplastic disease has not been described. Such a method would greatly advance our understanding of disease processes, and accelerate the development of effective intervention strategies.

Photoproteins such as luciferase from the firefly, *Photinus pyralis*, have been used as reporter genes in both *in vitro* and *ex vivo* assays [12,13]. This luciferase has been used to study gene expression in cancer cell lines in culture [14,15], and to tag tumor cells for the purpose of monitoring growth and response to therapy in animal models of human disease [16,17]. However, analysis of *in vivo* cell proliferation in these studies was performed using an *ex vivo* assay. Evaluation of reporter gene expression following removal of tumor tissues is limited by the loss of both the contextual influences of intact organ systems, and most of the temporal information. We have previously demonstrated that internal bioluminescent signals from bacteria and cells of transgenic mice can be detected noninvasively, even when located at deep tissue sites in mice [18,19]. This contrasts other optical-imaging strategies that use external light sources to interrogate tumor tissue using inherent optical signatures, or concentration of exogenous dyes at tumor sites [4]; for review see Chance et

Address all correspondence to: Dr. Christopher H. Contag, School of Medicine, Stanford University, Stanford, CA 94305. E-mail: ccontag@cmgm.stanford.edu

Received 9 August 1999; Accepted 18 August 1999.

al. [20]. Photons, originating from photoproteins as internal biological sources of light, that are transmitted through mammalian tissues reveal spatial and temporal information relative to the labeled cells [21].

In this study, we have extended our use of optical reporter genes to include *in vivo* monitoring of tumor cell lines labeled through constitutive expression of luciferase, and noninvasively assessing cellular proliferation in animal models. A stable reporter cell line of HeLa cells (HeLa-*luc*) was generated through selection of an integrated reporter construct consisting of a portion of the viral promoter from SV-40 driving expression of a modified luciferase gene that has been optimized for mammalian expression [13,22]. HeLa-*luc* cells were introduced into animals via subcutaneous, intraperitoneal and intravenous inoculation. The kinetics of cellular proliferation of labeled cells in irradiated severe combined immunodeficiency (SCID) mice was noninvasively assessed using an intensified charge coupled device (ICCD) camera to generate whole body images. The signals from labeled cells in these whole body images were used to both rapidly localize tumors and quantify cellular proliferation. The dynamic range of this assay permitted the study of disease from early to late stages.

Our demonstrated ability to detect small numbers of tumor cells in living animals noninvasively will permit the assessment of therapies designed to treat minimal disease states. Minimal residual disease after elimination of the tumor mass often results in relapse of disease, and remains a major therapeutic challenge. In addition, as diagnostic tests improve, therapies directed at minimal disease states early in the disease course will need to be developed. The approach described here can accelerate development of such therapeutic strategies by providing a rapid *in vivo* assay for therapeutic efficacy that is inexpensive and accessible. Imaging approaches in general will improve the predictability of animal models of human neoplastic disease by providing spatiotemporal information, but the ease and versatility of the approach described here will result in high throughput animal models for drug discovery.

Methods

Transfection of Tumor Cell Lines

The human cervical carcinoma line, HeLa, was transfected with the plasmid vector, pGL3 (Promega Corp., Madison, WI). This vector encodes a modified firefly luciferase gene under the control of the SV-40 promoter [13,22]. The pGL3 control plasmid along with the pZeo-SV2 vector (Invitrogen, San Diego, CA) [23], which confers resistance to the bleomycin analog, Zeocin (Invitrogen), were cotransfected into HeLa cells using the liposome formulation Lipofectamine (Gibco BRL Gaithersburg, MD), according to the manufacturer's instructions. Optimal conditions for DNA delivery were identified by adding luciferin (0.15 mg/ml final concentration; BioSynth, Naperville, IL) to the cell culture medium. Stable transfectants were selected in Zeocin (Invitrogen; 500 μg/ml) and light emission was utilized to screen cultures for expression of the reporter gene using an intensified charge coupled device (ICCD) camera (C2400-32, Hamamatsu, Japan). Colonies of cells emitting light were grown in Dulbecco's modified Eagle's medium (DMEM) supplemented with penicillin (100 U/ml), streptomycin (100 μg/ml), glutamine (2 mmol), 2-mercaptoethanol (50 μg/ml) fetal calf serum (FCS, 10%; Hyclone Labs, Logan, UT) and Zeocin (Invitrogen; 500 μg/ml). Stable cell lines are referred to as HeLa-*luc* cells.

Immunodeficient Mice

CB17 SCID mice 8–12 weeks old were obtained from the colony at Stanford University. From birth, mice were housed in a clean environment and fed autoclaved food and water containing trimethoprim sulfamethoxazole (Biocraft, Elmwood Park, NJ). One day prior to injection of the tumor cells, the animals were radiated with 200 cGy whole body radiation to limit endogenous natural killer (NK) cell activity [24]. Mice were injected with HeLa-*luc* tumor cells at the indicated cell dose and route of administration in 50–200 μl total volume (IV at 50 μl). All animal experiments were performed under protocols approved by the Institutional Animal Care and Use Committee at Stanford University.

Imaging of Tumor Xenografts

An aqueous solution of luciferin (BioSynth; 150 mg/ml) was injected into the peritoneal cavity of mice 5 minutes prior to imaging (150 mg/kg body weight). The concentration of luciferin used in the present study was previously selected using a transgenic model where expression of a luciferase transgene was at a tissue site, skin, distant from the site of substrate administration, peritoneal cavity [19]. In the skin expression model, optimal signal intensity was obtained with 150 mg/kg suggesting that substrate was in excess, and peak signal was obtained at 5–20 minutes post administration of the substrate.

Prior to imaging, mice were sedated with i.p. injections of pentobarbital (50 mg/kg). A grayscale body surface reference image was collected in a light-tight chamber with the chamber door slightly ajar. The chamber door was then closed to exclude room light, and photons emitted from within the animal and transmitted through the tissue were collected. For this purpose, a low light imaging system comprised of an ICCD camera fitted with a 50-mm f1.2 Nikkor lens (Nikon, Japan) and computer with image-analysis capabilities were used. Integration times were for a period of 5 minutes.

A pseudocolor image representing light intensity (blue least intense and red most intense) was generated on an Argus 20 image processor (Hamamatsu); images were transferred using a plug-in module (Hamamatsu) to a computer (Macintosh 8100/100, Apple Computer, Cupertino, CA) running an image processing application (Photoshop, Adobe, Mountain View, CA). Grayscale reference images and pseudocolor images were superimposed using the image-processing software, and annotations were added using another graphics software package (Canvas Version 5.0, Deneba, Miami, FL). For those animals with extensive

tumor signal a display range of 0–7 bits is shown to better localize the tumor signal, otherwise images are shown at the bit range of 0–3 (lowest setting).

Results

As few as 30 HeLa-*luc* could be detected in culture using the ICCD camera system (unpublished data). The ability to detect a small number of cells in culture suggested that we may be able to use this ICCD camera with the same optics to detect cells in living animal models. Therefore, this stable line was injected into irradiated SCID mice using several different routes, and proliferation of the HeLa-*luc* cells was evaluated. Whole body images, for each animal, were obtained at weekly intervals over a 28-day time course.

Immediately following i.p. injection of 1×10^4 HeLa-*luc* cells (day 0), tumor signals distributed over the entire abdominal area were detected (Figure 1*A*). By day 7, signals in the animals that received low doses were reduced and discrete sites of photon emission were observed in a majority of the animals. Tumor signals increased significantly over the next 28-day period with exponential growth in the peritoneal cavity. By day 14, several large areas of tumor growth were apparent and by day 21 signal was apparent from the entire abdominal area. At day 21, light emission was intense; images of these signals are presented at a different bit range to permit localization of the signal source. No apparent signals were detected from sites other than the peritoneal cavity. Thus, the HeLa-*luc* cells did not appear to metastasize to sites beyond site of injection. Despite the dramatic increases in tumor signal, the animals appeared functionally normal without any evidence of overt disease.

Using this *in vivo* model the growth of the tumor could be directly visualized and quantified. Serial images were obtained over the 28-day time course for all animals, and the mean photon counts determined and plotted for each animal or injection site (Figure 1*B*). Following i.p. injection of the tumor cells, exponential growth of the tumor was observed for each dose of HeLa-*luc* cells. Evidence of tumor

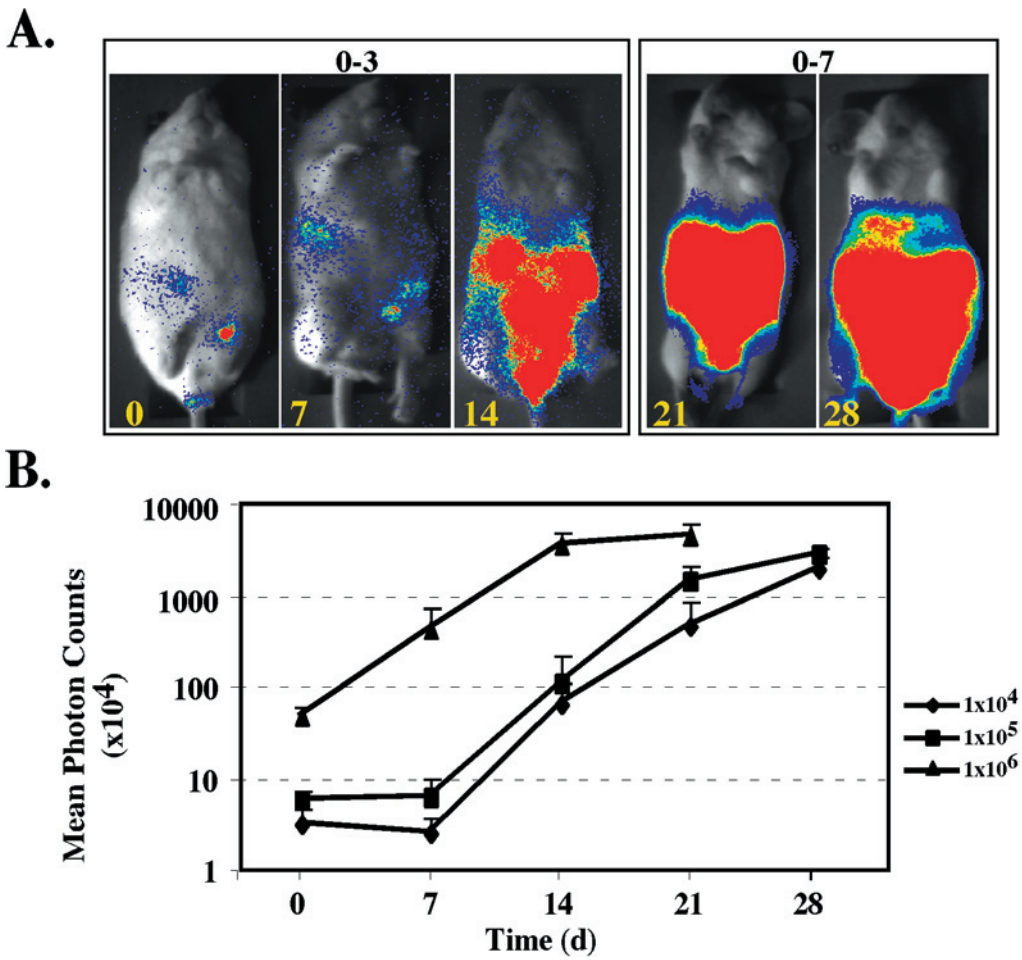

Figure 1. *Kinetics of tumor cell growth following intraperitoneal injection of tumor cells. HeLa-luc cells were injected into SCID mice and the animals were imaged weekly for 28 days. (A) One representative animal injected with 1×10^5 HeLa-luc cells is shown. Substrate was administered IP and signals were obtained with 5 minute integration times. Days 0 to 14 are displayed at a 0–3 bit range, days 21 and 28 at the less sensitive 0–7 bit range to optimize anatomical localization. (B) Quantification of tumor signals was obtained for the three cell concentrations tested. Data are plotted as mean photon counts from three animals per group, with respect to time.*

growth was obtained early (14 days), long before the animals demonstrated evidence of disease. By 28 days after injection, the tumor signal was between 100- to 1000-fold greater than that observed at the time of initial injection. At the lower cell doses, the tumor signal did not begin to rise until 14 days after injection and was associated with the formation of discrete sites of signal.

Animals were also studied following subcutaneous (SC) injection of the HeLa-*luc* cells at concentrations of 1×10^4, 1×10^5 and 1×10^6 cells at each of four discrete sites on the dorsum of each animal. Animals which received 1×10^6 or 1×10^4 HeLa-*luc* cells are shown in Figure 2*A* and 2*B*, respectively. The signal from each of the sites of injection were quantified and plotted (Figure 2*C*). Clear, quantifiable images were observed with as few as 1×10^4 HeLa-*luc* cells immediately after injection, and temporal analyses demonstrated increased tumor signals over the 28-day observation period. There was no apparent signal detected beyond the sites of injection. Thus, the HeLa-*luc* cells did not appear to metastasize at this site either, but instead proliferated at the sites of injection. Some variation in tumor signal was

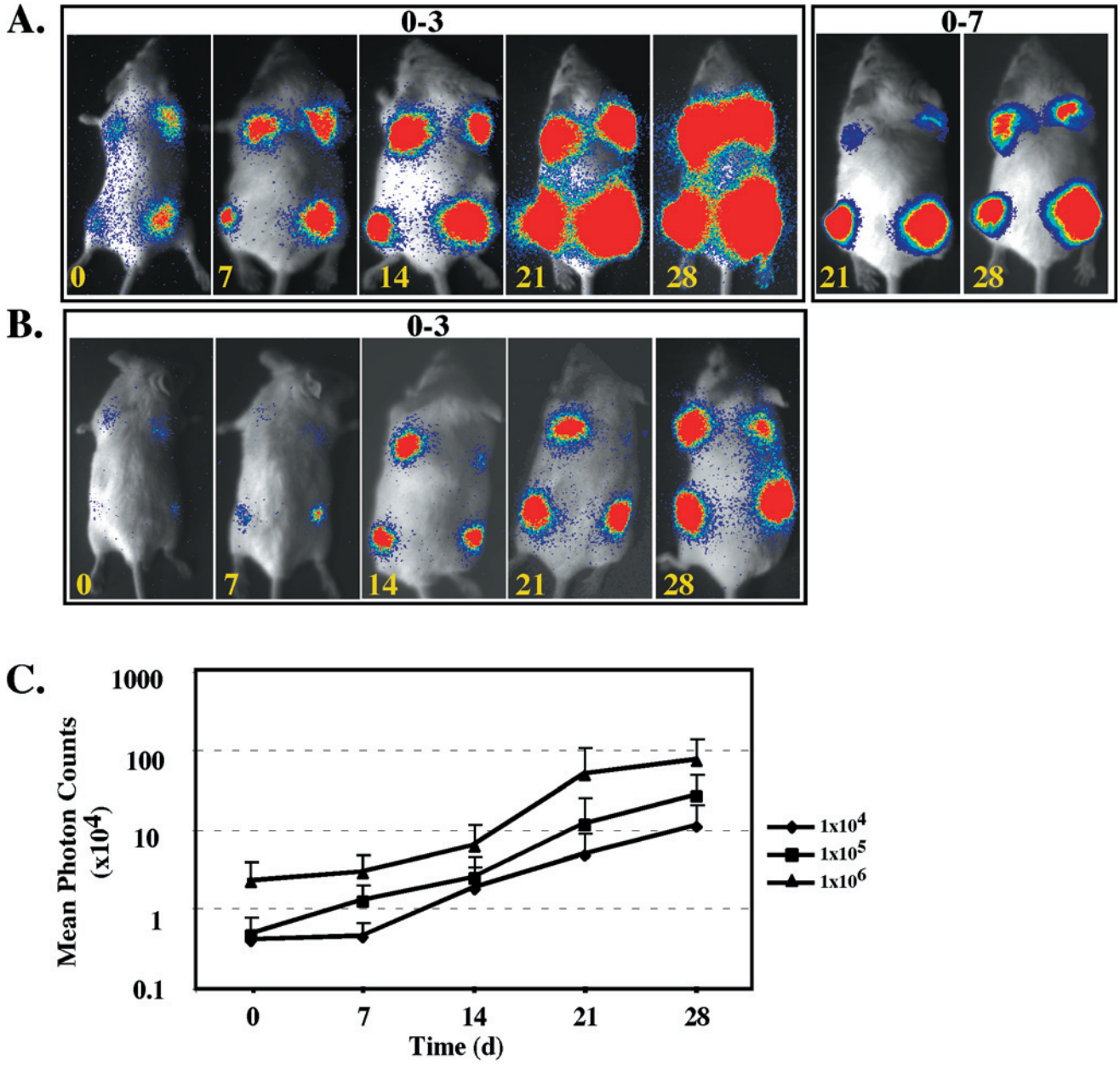

Figure 2. *Temporal analysis of tumor cell growth at subcutaneous sites. HeLa-luc cells were injected at four discrete sites on the dorsum of each of three SCID mice at concentrations of 1×10^6 (A) or 1×10^4 cells per site (B). Data were obtained on the day of injection and serially every 7 days until day 28. Images are presented at a bit range of 0–3. Additionally, images of the mouse injected with 1×10^6 cells are also displayed at the less sensitive 0–7 bit range for better anatomical localization of the signal source. Quantification of the tumor signals was obtained for each injection site, and the data plotted as mean photon counts, with respect to time (C). Data were obtained with 5 minutes integration times. These data indicated that growth kinetics of the HeLa-luc cells could be monitored at subcutaneous sites over time.*

observed following SC injection. This variation persisted over the 28-day period and likely represented variability at the time of injection. Nonuniformity of spread of tumor cells at the injection site may also explain this result.

The kinetics of tumor cell growth could be quantified following SC injection (Figure 2*C*). All animals that received SC injections of tumor cells appeared functionally normal throughout the 28-day observation period, and tumor nodules were not apparent by palpation. The absence of palpable nodules, even for animals that received injections of 1×10^6 cells, further indicated that this *in vivo* assay is extremely sensitive. Dramatic increases in tumor signal were observed long before the animals exhibited any evidence of overt tumor cell growth using more conventional measures such as the formation of palpable nodules, malaise, and death. The assay has a dynamic range that offers the possibility of following tumor growth over many orders of magnitude.

Animals receiving HeLa-*luc* cells via IV injection required large numbers of cells for successful engraftment. Three different cell doses of 1×10^6, 5×10^6, and 1×10^7 cells were evaluated in triplicate and representative animals are shown (Figure 3). Two days after the injection of HeLa-*luc* cells, signals were initially seen over the lungs. An animal that received 1×10^7 cells had detectable signal distributed over the entire animal with greatest intensity over the lungs. Signals from the lungs persisted for 7 days in animals that received more than 1×10^6 HeLa-*luc* cells. Signals at other sites including the head and tail were apparent in animals that received doses of 5×10^6 cells or greater. Engraftment of the HeLa-*luc* cells in the animals that received cells via IV administration was less reliable than i.p. or SC routes of administration, with detectable signals in only one of three animals following IV administration compared to all of the animals that received cells via other routes.

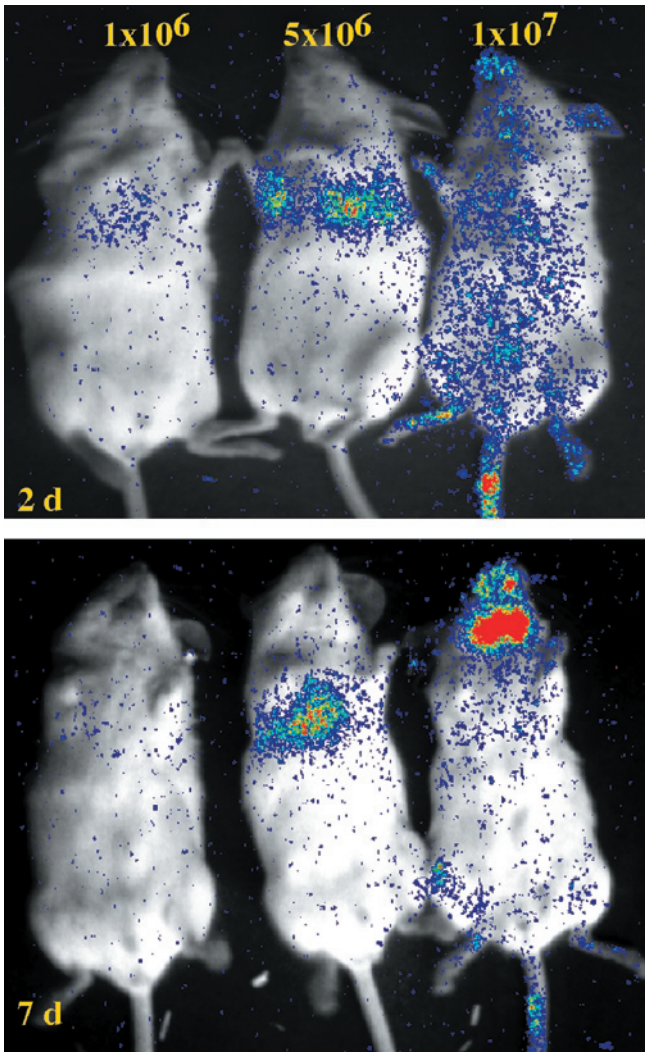

Figure 3. *Localization of tumor signal following intravenous injection. Representative animals that received between 1×10^6 and 1×10^7 HeLa-luc cells via IV injection are shown. Signals were apparent from the lungs initially, and then at a variety of anatomical sites at later times. Images, displayed here at a bit range of 0–3, were obtained at 2 and 7 days after injection of cells.*

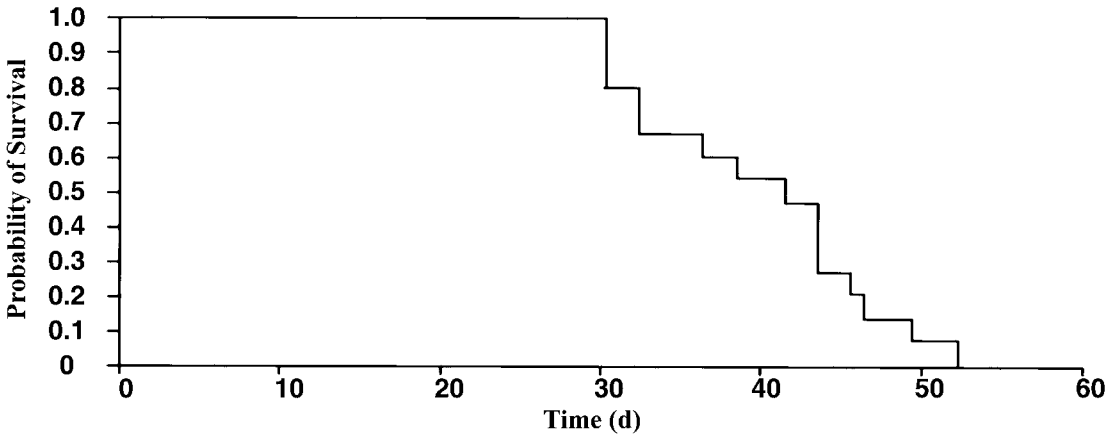

Figure 4. *Probability of survival of SCID mice bearing the HeLa-luc tumor. The survival of 15 SCID mice following IP injection of 1×10^4 HeLa-luc cells was monitored over time.*

Tumor cell growth could be monitored immediately following injection of tumor cells, via each of the three routes, with good sensitivity, and tumor cells could be detected before any overt signs of neoplastic disease. For example, following i.p. injection of 1×10^4 HeLa-*luc* cells, detectable signals were apparent through the entire study period, including the time of injection, and yet the animals did not succumb to the growth of the HeLa-*luc* cells until after 40–50 days (Figure 4). This imaging strategy provides access to quantitative data through the entire disease course.

Discussion

The development of real-time noninvasive, and minimally invasive, assays for monitoring the progression of neoplastic disease in living systems would offer great benefit for the analyses of host response to disease, as well as in the testing of novel therapeutic strategies [25]. *In vivo* monitoring of optical reporter genes as indicators of expression had previously been limited to cell culture, embryos, plants and small nearly transparent animals such as flies and worms. Scanning techniques such as MRI and CT are modalities ideally suited to reveal structural information, although methods for acquiring functional data using MRI have been developed. MR imaging, however, requires long scan times and expensive instrumentation. PET imaging provides metabolic information and some reporter genes that concentrate radionuclides are available [7,9–11,26,27]. However, PET is limited by the requirement of radioactive tracers with relatively short half-lives.

Biochemical and molecular assays such as the polymerase chain reaction (PCR) are sensitive and specific; however, these are time consuming and are severely constrained by sampling limitations [28]. Moreover, a single animal cannot be easily evaluated over time, and animals may need to be sacrificed at serial time points to gain good temporal analyses with statistical endpoints [29,30]. The large number of animals for these *ex vivo* studies can be technically difficult to handle and are prohibitively expensive. A variety of vital dyes have been utilized which have utility *in vivo* for tracking cell populations; however, since these agents are not produced by the cell and replicated with the chromosomal DNA they are generally washed out, or diluted out with cell division. Thus, such agents are limited and may not be suitable for imaging biological processes that occur over protracted time periods in adult animals [31].

Tagging of biological processes with reporters, which can be monitored and quantified externally provides a powerful tool for evaluating disease progression and response to therapy. In our oncology models we have utilized the optical reporter gene luciferase, which is a modified version of that isolated from the firefly *P. pyralis*. This reporter is well suited for these studies since there is essentially no background as other sources of significant bioluminescence are not present in mammals. This contrasts the use of fluorescent tags where tissue autofluorescence and photobleaching can be extremely limiting. Fluorescent reporter genes require the use of excitation light, typically of short wavelengths, and emit in the green region of the spectrum. These wavelengths do not penetrate tissue well and signals from deep tissue sites may not be accessible. The luciferase enzyme produces light in the presence of the substrate luciferin, oxygen and ATP [12]; the light produced penetrates mammalian tissues, and can be externally detected and quantified using sensitive light imaging systems [21]. The reporter gene, which is introduced into the chromosomes of the target cells as a stable integration, is replicated with cell division and not lost over time. Images can be produced which provide spatial information and the animals repeatedly imaged which provides temporal information. This ability to produce spatiotemporal data can be used to generate animal models of neoplastic disease that are more predictive of response to therapy and effects of experimental manipulation.

In this report, as few as 1×10^3 HeLa-*luc* cells could be visualized following i.p. injection, and tumor progression followed temporally. Growth proceeded in an exponential fashion such that by 28 days a dramatic increase in signal intensity was observed. Despite the signal observed over the

28-day time period these animals remained relatively robust and did not succumb to the tumor for an additional 30 days. Therefore, exponential growth of the tumor could be directly visualized noninvasively, and quantified over the entire body mass of the recipient animal. Similar observations were made following SC injection of the tumor cells where up to four discrete areas of tumor cell growth could be detected and quantified. HeLa-*luc* cells did not appear to metastasize following i.p. or SC injection and instead grew locally. Using this approach it is possible to study the growth of tumor cells at individual locations, and may also be used to evaluate the potential for metastasis.

There were differences in the sensitivity of detecting labeled cells at each of the three sites tested, and this was likely related to either greater distribution of cells, or metabolic activity at each site. Subcutaneous sites are likely constrained for both oxygen, a requirement for the luciferase enzymatic reaction, and space. It is possible that these constraints limited the signal intensity following SC injection compared to i.p. injection of tumor cells. Hypoxia will likely limit the luciferase reaction, and may alter the ability to quantify total cell numbers as the tumor mass increases. However, use of luciferase as a metabolic indicator may provide some insights into the growth of larger tumors and the propensity of cells at hypoxic sites to metastasize. Combination of MRI and luciferase imaging may be a useful way to obtain both tumor volume and data on metabolic activity for large tumors. When the cells are injected IV they circulate throughout the animal, and are distributed over a larger volume. It is anticipated that greater distribution of the signal in tissues of varied optical properties may account for our inability to detect fewer than 1×10^6 cells following IV injection.

Among the available imaging modalities for use in laboratory animals, only photoprotein imaging currently has the sensitivity to detect the small numbers of cells present in models of minimal disease states. However, optical reporters are limited by tissue penetration to several centimeters of tissue, and there is a loss of resolution with greater tissue depth. It is reasonable that combined imaging strategies can be used to compensate for limitations of individual imaging modalities. Optical methods, including photoprotein imaging, are well suited to complement other imaging modalities since optical methods tend to be less expensive and provide data not otherwise available. For example, monitoring tumor cells labeled with optical reporter genes may serve as a method to direct MRI investigation by providing a rapid prescreen. The speed and versatility of optical methods suggests that these methods can be used in the development of more versatile MRI reporter genes and imaging strategies. It is likely that combined reporter gene cassettes that provide MRI and optical signatures will be developed for combined imaging strategies.

The strength of PET and MRI in imaging of neoplastic disease is that each of these imaging modalities is currently available for human imaging, and the protocols that are being developed for *in vivo* cellular and molecular analyses could be applied to clinical investigation. The use of these modalities for monitoring patient response to therapy would offer clinicians great insight for effective management of neoplastic disease.

The model systems and method of detection described in this report will offer tremendous advantages for the study of both gene expression, in tumor and host cells, and response to therapy [19]. The ability to rapidly evaluate response to a therapeutic intervention *in vivo* in a quantitative fashion is an attribute of this approach. Since tumor cell growth in individual animals can be quantitatively assessed, the time and number of animals required can be greatly reduced. The sensitivity of detecting tumor cells labeled with photoprotein reporter genes may allow us to effectively shift the investigation of antineoplastic therapies from those that act on large numbers of cells to minimal disease models. This would permit the development of effective therapies with reduced toxicity to patients.

Acknowledgements

This work was funded in part through grants from a Translational Award from The Leukemia Society (6090-99), the National Cancer Institute (R01 CA80006), and unrestricted gifts from the Mary L. Johnson and Hess Research Funds. M.E. was supported by a grant from the Mildred Scheel Cancer Research Foundation.

References

[1] Ross BD, Zhao Y-J, Neal ER, Stegman LD, Ercolani M, Ben-Yoseph O, and Chenevert TL (1998). Contributions of cell kill and posttreatment tumor growth rates to the repopulation of intracerebral 9L tumors after chemotherapy: an MRI study. *Proc Natl Acad Sci USA* **95**, 7012–7017.

[2] Galons J-P, Altbach MI, Paine-Murrieta GD, Taylor CW, and Gillies RJ (1999). Early increases in breast tumor xenograft water mobility in response to paclitaxel therapy detected by non-invasive diffusion magnetic resonance imaging. *Neoplasia* **1**, 113–117.

[3] Jacobs A, Dubrovin M, Hewett J, Sena-Esteves M, Tan C-W, Slack M, Sadelain M, Breakefield XO, and Tjuvajev JG (1999). Functional coexpression of HSV-1 thymidine kinase and green fluorescent protein: implications for noninvasive imaging of transgene expression. *Neoplasia* **1**, 154–161.

[4] Weissleder R, Tung CH, Mahmood U, and Bogdanov A, Jr. (1999). *In vivo* imaging of tumors with protease-activated near-infrared fluorescent probes. *Nat Biotechnol* **17** (4): 375–378.

[5] Bogdanov A, Jr., and Weissleder R (1998). The development of *in vivo* imaging systems to study gene expression. *Trends Biotechnol* **16** (1): 5–10.

[6] Chenevert TL, McKeever PE, and Ross BD (1997). Monitoring early response of experimental brain tumors to therapy using diffusion magnetic resonance imaging. *Clin Cancer Res* **3** (9): 1457–1466.

[7] Tjuvajev JG, Avril N, Oku T, Sasajima T, Miyagawa T, Joshi R, Safer M, Beattie B, DiResta G, Daghighian F, Augensen F, Koutcher J, Zweit J, Humm J, Larson SM, Finn R, and Blasberg R (1998). Imaging herpes virus thymidine kinase gene transfer and expression by positron emission tomography. *Cancer Res* **58** (19): 4333–4341.

[8] Uehara H, Miyagawa T, Tjuvajev J, Joshi R, Beattie B, Oku T, Finn R, and Blasberg R (1997). Imaging experimental brain tumors with 1-aminocyclopentane carboxylic acid and alpha-aminoisobutyric acid: comparison to fluorodeoxyglucose and diethylenetriaminepentaacetic acid in morphologically defined tumor regions. *J Cereb Blood Flow Metab* **17** (11): 1239–1253.

[9] Tjuvajev JG, Finn R, Watanabe K, Joshi R, Oku T, Kennedy J, Beattie B, Koutcher J, Larson S, and Blasberg RG (1996). Noninvasive imaging of herpes virus thymidine kinase gene transfer and expression: a

potential method for monitoring clinical gene therapy. *Cancer Res* **56** (18): 4087–4095.

[10] Gambhir SS, Barrio JR, Herschman HR, and Phelps ME (1999). Imaging gene expression: principles and assays. *J Nucl Cardiol* **6** (2): 219–233.

[11] Gambhir SS, Barrio JR, Phelps ME, Iyer M, Namavari M, Satyamurthy N, Wu L, Green LA, Bauer E, MacLaren DC, Nguyen K, Berk AJ, Cherry SR, and Herschman HR (1999). Imaging adenoviral-directed reporter gene expression in living animals with positron emission tomography. *Proc Natl Acad Sci USA* **96** (5): 2333–2338.

[12] Hastings JW (1996). Chemistries and colors of bioluminescent reactions: a review. *Gene* **173** (1): 5–11.

[13] Wood KV (1995). Marker proteins for gene expression. *Curr Opin Biotechnol* **6** (1): 50–58.

[14] Willard ST, Faught WJ, and Frawley LS (1997). Real-time monitoring of estrogen-regulated gene expression in single, living breast cancer cells: a new paradigm for the study of molecular dynamics. *Cancer Res* **57** (20): 4447–4450.

[15] Chen H, Biel MA, Borges MW, Thiagalingam A, Nelkin BD, Baylin SB, and Ball DW (1997). Tissue-specific expression of human achaete-scute homologue-1 in neuroendocrine tumors: transcriptional regulation by dual inhibitory regions. *Cell Growth Differ* **8** (6): 677–686.

[16] Takakuwa K, Fujita K, Kikuchi A, Sugaya S, Yahata T, Aida H, Kurabayashi T, Hasegawa I, and Tanaka K (1997). Direct intratumoral gene transfer of the herpes simplex virus thymidine kinase gene with DNA-liposome complexes: growth inhibition of tumors and lack of localization in normal tissues. *Jpn J Cancer Res* **88** (2): 166–175.

[17] Zhang L, Hellstrom KE, and Chen L (1994). Luciferase activity as a marker of tumor burden and as an indicator of tumor response to antineoplastic therapy *in vivo*. *Clin Exp Metastasis* **12**, 87–92.

[18] Contag CH, Contag PR, Mullins JI, Spilman SD, Stevenson DK, and Benaron DA (1995). Photonic detection of bacterial pathogens in living hosts. *Mol Microbiol* **18** (4): 593–603.

[19] Contag CH, Spilman SD, Contag PR, Oshiro M, Eames B, Dennery P, Stevenson DK, and Benaron DA (1997). Visualizing gene expression in living mammals using a bioluminescent reporter. *Photochem Photobiol* **66** (4): 523–531.

[20] Chance B, Luo Q, Nioka S, Alsop DC, and Detre JA (1997). Optical investigations of physiology: a study of intrinsic and extrinsic biomedical contrast. *Philos Trans R Soc London Ser B* **352** (1354): 707–716.

[21] Contag PR, Olomu IN, Stevenson DK, and Contag CH (1998). Bioluminescent indicators in living mammals. *Nat Med* **4** (2): 245–247.

[22] Sherf B, and Wood KV (1994). Firefly luciferase engineered for improved genetic reporting. *Promega Notes Magazine* **49**, 14–21.

[23] Calmels TP, Mistry JS, Watkins SC, Robbins PD, McGuire R, and Lazo JS (1993). Nuclear localization of bacterial *Streptoalloteichus hindustanus* bleomycin resistance protein in mammalian cells. *Mol Pharmacol* **44** (6): 1135–1141.

[24] Shpitz B, Chambers CA, Singhal AB, Hozumi N, Fernandes BJ, Roifman CM, Weiner LM, Roder JC, and Gallinger S (1994). High level functional engraftment of severe combined immunodeficient mice with human peripheral blood lymphocytes following pretreatment with radiation and anti-asialo GM1. *J Immunol Methods* **169** (1): 1–15.

[25] Hirsch-Ginsberg C (1998). Detection of minimal residual disease: relevance for diagnosis and treatment of human malignancies. *Annu Rev Med* **49**, 111–122.

[26] Tjuvajev JG, Stockhammer G, Desai R, Uehara H, Watanabe K, Gansbacher B, and Blasberg RG (1995). Imaging the expression of transfected genes *in vivo*. *Cancer Res* **55** (24): 6126–6132.

[27] Gambhir SS, Barrio JR, Wu L, Iyer M, Namavari M, Satyamurthy N, Bauer E, Parrish C, MacLaren DC, Borghei AR, Green LA, Sharfstein S, Berk AJ, Cherry SR, Phelps ME, and Herschman HR (1998). Imaging of adenoviral-directed herpes simplex virus type 1 thymidine kinase reporter gene expression in mice with radiolabeled ganciclovir. *J Nucl Med* **39** (11): 2003–2011.

[28] Negrin RS, and Blume KG (1991). The use of the polymerase chain reaction for the detection of minimal residual malignant disease. *Blood* **78** (2): 255–258.

[29] Uckun FM, Sather H, Reaman G, Shuster J, Land V, Trigg, M, Gunther R, Chelstrom L, Bleyer A, and Gatynon P (1995). Leukemic cell growth in SCID mice as a predictor of relapse in high- risk B-lineage acute lymphoblastic leukemia. *Blood* **85** (4): 873–878.

[30] Uckun FM (1996). Severe combined immunodeficient mouse models of human leukemia. *Blood* **88** (4): 1135–1146.

[31] Hendrikx PJ, Martens CM, Hagenbeek A, Keij JF, and Visser JW (1996). Homing of fluorescently labeled murine hematopoietic stem cells. *Exp Hematol* **24** (2): 129–140.